Localization in light nuclei

P.-G. Reinhard,[1] J. A. Maruhn,[2] A. S. Umar,[3,*] and V. E. Oberacker[3]
[1]*Institut für Theoretische Physik, Universität Erlangen, D-91054 Erlangen, Germany*
[2]*Institut für Theoretische Physik, Goethe-Universität, D-60438 Frankfurt am Main, Germany*
[3]*Department of Physics and Astronomy, Vanderbilt University, Nashville, Tennessee 37235, USA*
(Received 1 November 2010; revised manuscript received 9 February 2011; published 14 March 2011)

We investigate the presence of spatial localization in nuclei using a method that maps the nucleon same-spin pair probability and is based on the density matrix. The method is used to study spatial localization of light nuclei within the Hartree-Fock approximation. We show that the method provides an alternative tool for studying spatial localization in comparison to the localization observed from maxima in the nuclear mass density.

DOI: 10.1103/PhysRevC.83.034312 PACS number(s): 21.60.Jz, 21.30.Fe, 21.60.Cs, 27.20.+n

I. INTRODUCTION

Clustering phenomena in light nuclei have always been an intriguing aspect of nuclear structure physics. Theoretical understanding of why and how conglomeration of nucleons to subunits within a nucleus results in an increase in stability remains an actively investigated question. In particular, α clustering in light nuclei has a long history [1–4] and suggests the existence of configurations resembling the formation of *nuclear molecules* [5–7]. It has also been suggested that neutron-rich isotopes of some light nuclei may give rise to new types of cluster structures [7,8]. Most of the theoretical analyses of cluster structures have been performed with *a priori* initialization in terms of clusters and effective interactions, which are determined so as to reproduce the binding energies and scattering phase shifts of these configurations. In contrast, nuclear structure calculations based on independent-particle approximation or density functionals also manifest cluster-like substructures as marked concentrations of density in the visualization of the total nuclear mass density. For example, Hartree-Fock (HF) calculations for light nuclei often show such formations [9], however, because the HF single-particle states are generally spread across the whole nucleus, they are delocalized, which makes the entanglement of these substructures in terms of single-particle orbitals very difficult. Furthermore, the identification of cluster and shell structures based only on the mass density may be an oversimplification, as it is missing other aspects of the many-body system, for example, the kinetic energy density or density gradients, which may help to provide a more detailed understanding of the underlying structure. Finally, with the rising popularity of the density functional approach in nuclear physics, it may be desirable to have a new localization measure that stems directly from the nuclear density matrix, as all of the information is contained in this quantity.

II. THE LOCALIZATION MEASURE

A. Outline of formalism

An alternative measure of localization had been developed in the context of a mean-field description for electronic systems [10]. A fermionic mean-field state is fully characterized by the one-body density matrix

$$\rho_{q\sigma\sigma'}(\mathbf{r},\mathbf{r}') = \sum_{\alpha\in q}\phi_\alpha(\mathbf{r}\sigma)\phi^*_\alpha(\mathbf{r}'\sigma'). \tag{1}$$

The probability of finding two nucleons with the same spin at spatial locations $\mathbf{r}$ and $\mathbf{r}'$ (same-spin pair probability) for isospin q is given by

$$P_{q\sigma}(\mathbf{r},\mathbf{r}') = \rho_{q\sigma}(\mathbf{r})\rho_{q\sigma}(\mathbf{r}') - |\rho_{q\sigma\sigma}(\mathbf{r},\mathbf{r}')|^2, \tag{2}$$

where $\rho_{q\sigma}(\mathbf{r}) = \rho_{q\sigma\sigma}(\mathbf{r},\mathbf{r})$ is the local density. The conditional probability of finding a nucleon at $\mathbf{r}'$ when we know with certainty that another nucleon with the same spin and isospin is at $\mathbf{r}$ is

$$R_{q\sigma}(\mathbf{r},\mathbf{r}') = \rho_{q\sigma}(\mathbf{r}') - \frac{|\rho_{q\sigma\sigma}(\mathbf{r},\mathbf{r}')|^2}{\rho_{q\sigma}(\mathbf{r})}. \tag{3}$$

Because we are interested in the localization aspects of this probability, it is sufficient to consider only the local short-range behavior of the conditional probability, which one can obtain by performing a spherical averaging over a shell of radius δ about the point $\mathbf{r}$ and then Taylor expanding the resulting expression to get [10]

$$R_{q\sigma}(\mathbf{r},\delta) \approx \frac{1}{3}\left(\tau_{q\sigma} - \frac{1}{4}\frac{[\nabla\rho_{q\sigma}]^2}{\rho_{q\sigma}} - \frac{\mathbf{j}^2_{q\sigma}}{\rho_{q\sigma}}\right)\delta^2 + \mathcal{O}(\delta^3), \tag{4}$$

where $\tau_{q\sigma}$ and $\mathbf{j}_{q\sigma}$ are the kinetic energy density and current density given by

$$\tau_{q\sigma}(\mathbf{r}) = \sum_{\alpha\in q}|\nabla\phi_\alpha(\mathbf{r}\sigma)|^2,$$

$$\mathbf{j}_{q\sigma}(\mathbf{r}) = \sum_{\alpha\in q}\mathrm{Im}[\phi^*_\alpha(\mathbf{r}\sigma)\nabla\phi_\alpha(\mathbf{r}\sigma)],$$

$$\nabla\rho_{q\sigma}(\mathbf{r}) = 2\sum_{\alpha\in q}\mathrm{Re}[\phi^*_\alpha(\mathbf{r}\sigma)\nabla\phi_\alpha(\mathbf{r}\sigma)].$$

The reason for writing $\nabla\rho_{q\sigma}$ explicitly is to emphasize that to have a smooth behavior of the quantities calculated below, it is essential to calculate all quantities directly from the wave functions. The expression shown in Eq. (4) suggests

*umar@compsci.cas.vanderbilt.edu

the definition of a localization measure,

$$D_{q\sigma}(\mathbf{r}) = \left(\tau_{q\sigma} - \frac{1}{4}\frac{[\nabla \rho_{q\sigma}]^2}{\rho_{q\sigma}} - \frac{\mathbf{j}_{q\sigma}^2}{\rho_{q\sigma}} \right), \tag{5}$$

which is also valid for time-dependent Slater determinants [11]. It is important to remember that $D_{q\sigma}$ is the short-range limit of the conditional like-spin *pair* probability and may contain correlations that are not evident in simple one-body observables, such as the mass density. The localization measure defined by Eq. (5) is a reverse relation, for example, the higher the probability of finding two like-spin particles in the vicinity of each other, the smaller the value of D. For this reason it is customary to define a reversed and normalized localization measure,

$$\begin{aligned} \mathcal{C}_{q\sigma}(\mathbf{r}) &= \left[1 + \left(\frac{\tau_{q\sigma}\rho_{q\sigma} - \frac{1}{4}[\nabla\rho_{q\sigma}]^2 - \mathbf{j}_{q\sigma}^2}{\rho_{q\sigma}\tau_{q\sigma}^{\mathrm{TF}}} \right)^2 \right]^{-1}, \\ \tau_{q\sigma}^{\mathrm{TF}} &= \frac{3}{5}(6\pi^2)^{2/3}\rho_{q\sigma}^{5/3}, \end{aligned} \tag{6}$$

where $\tau_{q\sigma}^{\mathrm{TF}}$ is the Thomas-Fermi kinetic energy density. The latter is used to provide a natural scale, which then allows the definition of a dimensionless measure. The current density vanishes in the static case, which we consider in the following.

B. Limiting cases and interpretation

This criterion, Eq. (6), is known in electronic systems as the electron localization function and it is used as one ingredient to analyze the bond structure of molecules in the static [10] and dynamic [11] domains. The information content of the localization function is understood by considering limiting cases.

The extreme case of ideal metallic bonding is realized for homogeneous matter where $\tau = \tau_{q\sigma}^{\mathrm{TF}}$. This yields $\mathcal{C} = \frac{1}{2}$, a value that thus signals a region with a nearly homogeneous Fermi gas as is typical for metal electrons, nuclear matter, or neutron stars. The opposite regime is space regions where exactly one single-particle wave function of type $q\sigma$ contributes. This is called *localization* in molecular physics. Such a situation yields $D_{q\sigma}(\mathbf{r}) = 0$, as it is not possible to find another like-spin state in the vicinity, and consequently, $\mathcal{C} = 1$, the value that signals *localization*. It should be noted that the localization function is invariant under unitary transformations among the single-particle wave functions in a Slater state [12]. In the nuclear case, it is the α particle that is perfectly localized in this sense, that is, that has $\mathcal{C} = 1$ everywhere for all states. Well-bound nuclei usually show metallic bonding and predominantly have $\mathcal{C} = \frac{1}{2}$. Light nuclei are often expected to contain pronounced α-particle substructures. Such a substructure means that in a certain region of space only an α particle is found, which in turn is signaled by $\mathcal{C} = 1$ in this region. In fact, an α substructure is a correlation of four particles: $p\uparrow$, $p\downarrow$, $n\uparrow$, and $n\downarrow$. Thus it is signaled only if we find simultaneously, for all four corresponding localization functions, $\mathcal{C}_{q\sigma} \approx 1$. In the following, we consider mainly $N = Z$ nuclei for which the four different particles have very similar wave functions. In this case, it suffices to consider, *pars pro toto*, only one localization function. Furthermore, it should be noted that a full identification of α-cluster substructures requires also checking the correlations among the four nucleons gathering in a "localized" region of the nucleus. The localization function is just the first step to identifying those regions, namely, the minimum necessary condition.

III. RESULTS AND DISCUSSION

In our calculations, the static HF equations are solved on a Cartesian three-dimensional mesh without any symmetry assumptions. The grid spacing was 1 fm, with a box size of $(-15.5, +15.5)$ fm in each dimension. The Skyrme energy functional was employed with the parametrization SkI3 [13]. The spatial derivatives are calculated using the fast Fourier transform and periodic boundary conditions are employed, except for the Coulomb potential, which is calculated with boundary conditions at infinity as described in Ref. [14].

A. Ground states of $N = Z$ nuclei

Figure 1 shows an x-z cut of the localization function, Eq. (6), for even-even $N = Z$ nuclei from $A = 4$ to $A = 20$. The left panel shows the proton localization criterion $\mathcal{C}_{p\uparrow}$ complemented in the right panel by the corresponding total density. As mentioned above, the states are spin symmetric, which yields identical localization plots for spin-up and spin-down. Moreover, for light $N = Z$ nuclei proton and neutron localizations are very similar owing to the small Coulomb interaction. (For neutron-rich isotopes this is no longer true, as we show below.) The color (gray-scale) coding is shown at the top of each column and remains the same throughout the column. The position of the density contour at half nuclear matter density ($\rho = 0.08$ fm^{-3}) is indicated by the color cyan in the maps of proton localization. One should keep in mind that the maxima and minima of the total nuclear density need not be correlated with those of the localization function, which is a topological quantity to describe localization (see also Fig. 2 and discussion thereof). The top panel in Fig. 1 shows the calculations for the ^{4}He nucleus. As we have described previously we see a perfect localization, with $\mathcal{C} = 1$ in all relevant regions where $\rho > 10^{-4}$ fm^{-3}. Lower densities lead to erroneous results for $\mathcal{C}$, owing to the very subtle cancellations required. The strongly prolate ^{8}Be shows a very distinct localization pattern, with perfect localization in the left and right halves of the contour plane and much smaller localization in the contact region where the wave functions overlap. As can be seen, this is much more pronounced in comparison to the total mass density plot. Here, it is probably reasonable to conclude that ^{8}Be can be considered an α-α molecule. With this version of the Skyrme force the ground state of ^{12}C is oblate deformed as shown in the right panel in Fig. 1. One may be tempted to consider this a planar arrangement of three α particles. A slight indication of that may be spotted in the localization plot. But it is not well developed, the configuration is too compact, and it shows preferably metallic binding, as we can see from the localization (left column), which stays

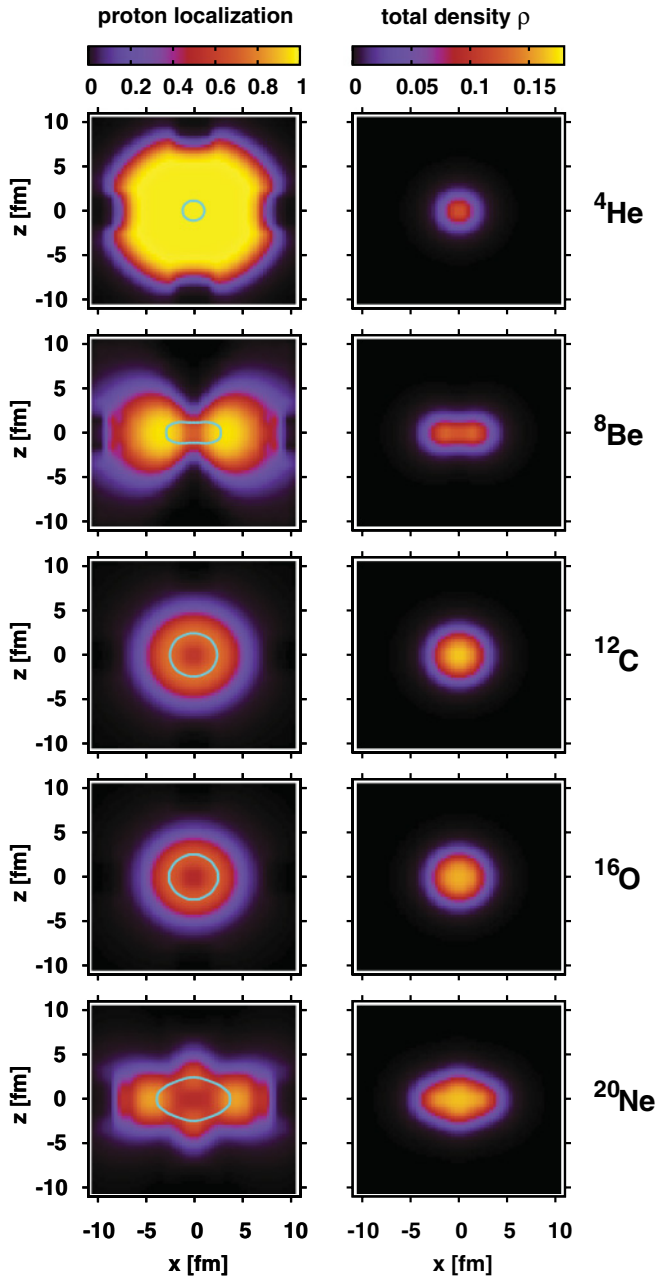

FIG. 1. (Color online) Color map (gray-scale) plots of proton localization (left column) and total density (in fm^{-3}; right column) for $Z = N$ nuclei up to ^{20}Ne. The position of the density contour at half nuclear matter density ($\rho = 0.08$ fm^{-3}) is indicated by the color cyan (light gray) in the maps of proton localization.

safely in a regime $\mathcal{C} \approx 1/2$. The strongly bound ^{16}O nucleus mostly shows a localization value of $\mathcal{C} = \frac{1}{2}$ throughout, as one would have expected. Its density is known to have a dip at the center [15]. This cannot be discriminated in the density plot here but can be observed as a region of lower localization in the localization map plot. To examine this further, we repeated the same calculation for ^{16}O using the SLy4 interaction [16]. In Fig. 2 we show a cut through the profile of the density and, similarly, through the localization function. We observe that the central dip in the total density is barely visible.

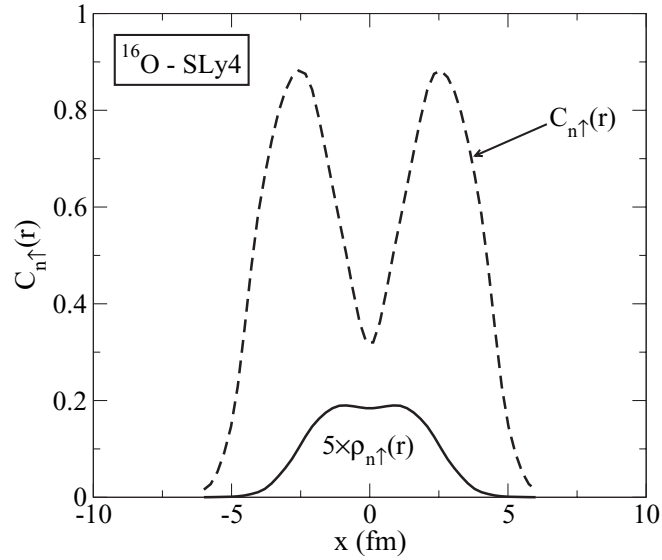

FIG. 2. Density profile and localization function for the ^{16}O nucleus.

The localization function, however, shows a very pronounced dip, indicating a strong and irreducible overlap of all wave functions in this center region. Note, furthermore, that the maxima of mass density and localization do not coincide. The localization has a preference toward the surface, where the lower density enhances the chance of finding one prevailing wave function.

Finally, the last panel in Fig. 1 shows results for the strongly prolate ^{20}Ne nucleus. The localization map shows two regions of high localization at the outer ends and a ring of somewhat enhanced localization at the center around the elongation axis. One can interpret this as a quasimolecular α-^{12}C-α configuration. The α substructures on both sides are almost as well developed as in ^{8}Be. We have also computed the further series of $N = Z$ nuclei, ^{24}Mg, ^{28}Si, ^{32}S, ^{36}Ar, and ^{40}Ca. These nuclei are increasingly compact and all show basically metallic binding similar to that of ^{12}C and ^{16}O shown here.

B. Strongly deformed configurations of light $N = Z$ nuclei

Very light $N = Z$ nuclei are likely to display isomeric, or at least transiently stable, configurations that are very elongated and resemble chains of α particles [20]. For somewhat heavier $N = Z$ one often finds shape coexistence with strongly prolate deformed nuclear configurations [21]. Such less bound and spatially more extended configurations are more likely to allow for α substructures. We thus have also considered such isomeric configurations for a number of light $N = Z$ nuclei. These configurations were found numerically by starting the static iteration from a sufficiently prolate configuration such that the iteration converged to the elongated isomeric state. Chain configurations were found immediately for ^{12}C and ^{16}O, while the heavier systems preferred to maintain a compact core between the α satellites. It is to be noted that these configurations are stable minima in a mean-field calculation. They may hybridize with the ground state in

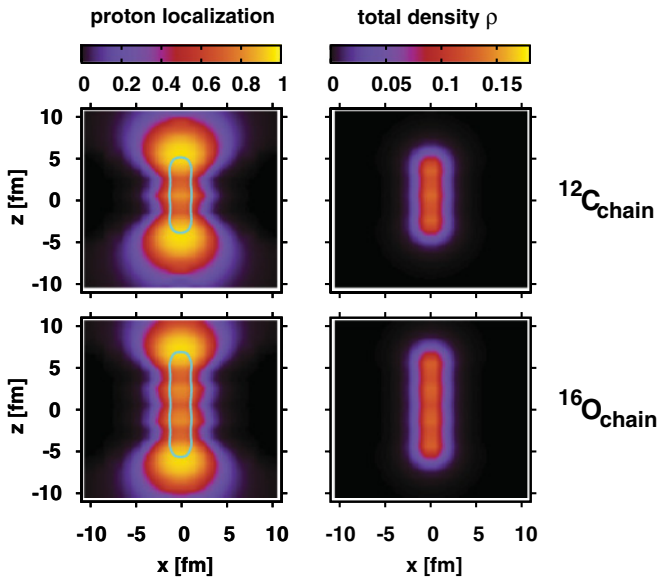

FIG. 3. (Color online) As Fig. 1, but for chain-like isomers of ^{12}C and ^{16}O.

correlated calculations. Still, such configurations may show up as transient configurations in nuclear reactions [20].

Figure 3 shows the total density and localization plots for the linear-chain states of ^{12}C and ^{16}O nuclei. For both, the density suggests an α-chain structure, which is, indeed, corroborated by the localization, which also shows three or four clearly separated maxima, $\mathcal{C} \approx 1$. The region of high localization is very large at both ends but much smaller for the maxima in the interior, owing to the larger wave-function overlap. One interesting point about the ^{12}C linear-chain configuration localization plot is that, in studying the dynamical formation of this chain state, as done in Ref. [17], we have observed that the dynamical vibrations of the mass density

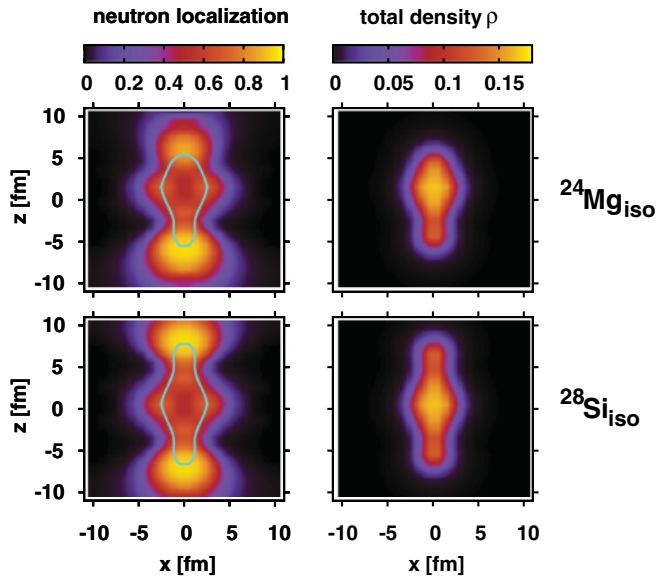

FIG. 4. (Color online) As Fig. 1, but for stretched isomers of ^{24}Mg and ^{28}Si.

resembled the localization plot with only the equilibrium shape having the triple-α structure. This is consistent with the kinetic interpretation of the localization function, suggesting that kinetic energies of the same-spin pairs peak mostly around the ends of the linear chain.

Figure 4 shows strongly prolate (not yet chain-like isomers, which lie higher in energy) isomers of ^{24}Mg and ^{28}Si. Unlike the compact ground-state configurations, these isomers indicate interesting molecular substructures. One may interpret ^{24}Mg as an α-^{12}C-α-α molecule and ^{28}Si as an α-α-^{12}C-α-α. Again, the outermost α's are best developed, with large regions of high localization. The inner α particles have already degraded localization owing to neighboring wave functions from both sides.

C. An example for $N > Z$: The ^{20}C chain

Recently, much interest has been devoted to the study of cluster configurations for neutron-rich isotopes of light nuclei [5,6,18]. In particular, the linear-chain configurations of C isotopes and their stability against bending modes has been of interest. For nuclei with $N > Z$, where proton and neutron wave functions are naturally different, the search for α substructure requires a simultaneous analysis of proton and neutron localization. To that end, we consider also as an α localization the combination $\sqrt{\mathcal{C}_{p\uparrow}\mathcal{C}_{n\uparrow}}$. The spin-up and spin-down wave functions are still degenerate such that it

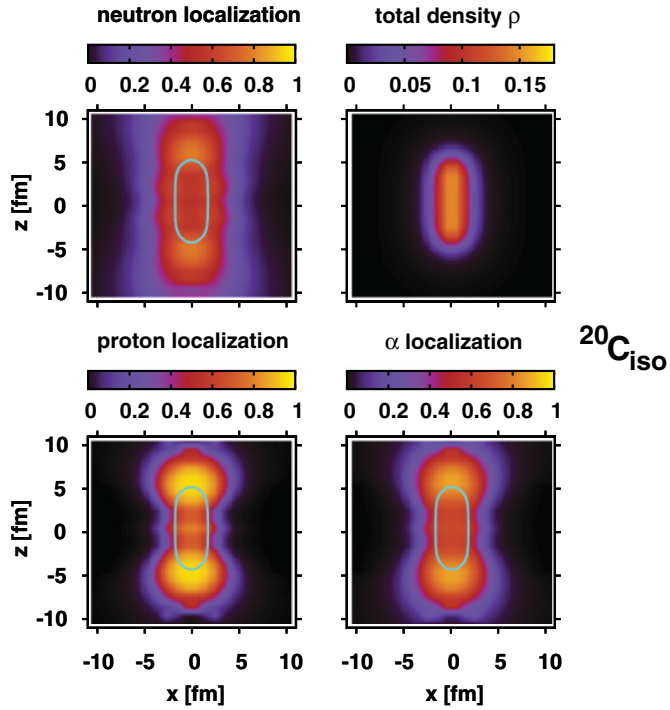

FIG. 5. (Color online) Color map plots of localizations and density for the linear-chain configuration of ^{20}C. Lower left: proton localization. Upper left: neutron localization. Lower right: α localization ($\equiv\sqrt{\mathcal{C}_{p\uparrow}\mathcal{C}_{n\uparrow}}$). Upper right: total density (in fm^{-3}). The position of the density contour at half nuclear matter density ($\rho = 0.08$ fm^{-3}) is indicated by cyan color (light gray) in the maps of localization.

suffices to consider one of the spins. In Fig. 5 we show proton, neutron, and α localization plots for the linear-chain isomer of the ^{20}C nucleus. As expected, owing to the neutron excess of ^{20}C the localization plots for neutrons and protons look considerably different. The protons show more distinct regions with high localization values in comparison to the neutron case, where the wave functions have more overlap owing to the large number of neutrons. The α localization is the obvious average of the two left panels. Despite the neutron cloud from the excess neutrons, some faint α substructure still appears at the edges of the chain. It is also interesting to observe that the total mass density does not show any pronounced features owing to the smoothing effect of the surplus neutrons, while the localization plots still reveal noteworthy structures.

IV. CONCLUSION

In summary, we have applied a localization measure that was developed originally for analyzing bonding structures in molecules to a study of α substructures in light nuclei. The localization function is obtained directly from the density matrix, in the mean-field approximation. It depends on the kinetic-energy density and current density, in addition to the mass density. It can be easily implemented for density functional theory calculations of nuclear structure. One of the fundamental reasons why the new localization measure is such an excellent predictor of correlation and localization is that it incorporates the kinetic energy of the relative motion of spin-parallel nucleons at a particular point in space, in addition to the mass density for the system [19]. In most cases this localization function shows more detailed localization or clustering features in comparison to the total mass density. Results for $N = Z$ nuclei up to ^{40}Ca show that pronounced localization, associated with α-particle substructures, appear only for the strongly prolate ground states of ^{8}Be and ^{20}Ne and, of course, trivially for ^{4}He. All other nuclei are more compact and show metallic binding. However, stretched isomers of light nuclei often show convincing α structures, particularly well developed for the α chains of ^{12}C and ^{16}O, but also for the prolate ^{24}Mg and ^{28}Si isomers. In the future we also plan to study the new localization function in time-dependent HF calculations of systems related to nuclear molecular configurations.

ACKNOWLEDGMENTS

This work was supported by the US Department of Energy under Grant No. DE-FG02-96ER40963 to Vanderbilt University and by the German BMBF under Contract Nos. 06FY9086 and 06ER142D.

[1] L. R. Hafstad and E. Teller, Phys. Rev. **54**, 681 (1938).
[2] H. Morinaga, Phys. Rev. **101**, 254 (1956).
[3] H. Horiuchi and K. Ikeda, Prog. Theor. Phys. **40**, 277 (1968).
[4] D. M. Brink and A. Weiguny, Nucl. Phys. A **120**, 59 (1968).
[5] N. Itagaki, S. Okabe, K. Ikeda, and I. Tanihata, Phys. Rev. C **64**, 014301 (2001).
[6] N. Itagaki, W. von Oertzen, and S. Okabe, Phys. Rev. C **74**, 067304 (2006).
[7] W. von Oertzen, M. Freer, and O. Kanada Enýo, Phys. Rep. **432**, 43 (2006).
[8] M. Ito, N. Itagaki, H. Sakurai, and K. Ikeda, Phys. Rev. Lett. **100**, 182502 (2008).
[9] J. A. Maruhn, N. Loebl, N. Itagaki, and M. Kimura, Nucl. Phys. A **833**, 1 (2010).
[10] A. D. Becke and K. E. Edgecombe, J. Chem. Phys. **92**, 5397 (1990).
[11] T. Burnus, M. A. L. Marques, and E. K. U. Gross, Phys. Rev. A **71**, 010501(R) (2005).
[12] A. Savin, J. Mol. Struct. Theochem. **727**, 127 (2005).
[13] P.-G. Reinhard and H. Flocard, Nucl. Phys. A **584**, 467 (1995).
[14] J. W. Eastwood and D. R. K. Brownrigg, J. Comput. Phys. **32**, 24 (1979).
[15] J. Friedrich and N. Vögler, Nucl. Phys. A **373**, 192 (1982).
[16] E. Chabanat, P. Bonche, P. Haensel, J. Meyer, and R. Schaeffer, Nucl. Phys. A **635**, 231 (1998); **643**, 441(E) (1998).
[17] A. S. Umar, J. A. Maruhn, N. Itagaki, and V. E. Oberacker, Phys. Rev. Lett. **104**, 212503 (2010).
[18] J. A. Maruhn, N. Loebl, A. S. Umar, N. Itagaki, M. Kimura, H. Horiuchi, and A. Tohsaki, Mod. Phys. Lett. A **25**, 1866 (2010).
[19] J. F. Dobson, J. Chem. Phys. **94**, 4328 (1991).
[20] P. E. Hodgson, Z. Phys. A **349**, 197 (1994).
[21] P.-G. Reinhard, D. J. Dean, W. Nazarewicz, J. Dobaczewski, J. A. Maruhn, and M. R. Strayer, Phys. Rev. C **60**, 14316 (1999).